Direct Tension and Split Basin Testing of 6-in. (150-mm)-Diameter Kubota Earthquake Resistant Ductile Iron Pipe

Submitted to:

Mr. Toshio Toshima
Kubota Corporation

by

Cornell University
School of Civil and Environmental Engineering
Cornell University
Hollister Hall
Ithaca, NY 14853

February, 2016

EXECUTIVE SUMMARY

Kubota has developed an earthquake-resistant ductile iron pipe (ERDIP), referred to as GENEX in Japan. Tests of 6-in. (150-mm)-diameter ERDIP pipe and pipeline section were performed at Cornell University to determine the capacity of the joint in direct tension and evaluate the ability of the jointed ductile iron pipeline to accommodate fault rupture. The testing was performed using the split-basin testing facility at Cornell University Large Scale Lifelines Testing Laboratory.

It should be noted that the term "rotation" in this report is equivalent to "deflection" as used commonly in the field and commercial pipeline information. Test results are summarized for direct joint tension, pipeline response to fault rupture, and significance of test results under the headings that follow.

Direct Joint Tension

A tension test was performed on a 6-in. (150-mm)-diameter Kubota ERDIP joint at a maximum internal pressure of 84 psi (579 kPa). The test began with the spigot fully inserted into the bell. As the pipe was pressurized, the spigot was displaced from the bell seat at approximately 9 psi (62 kPa) internal pressure. The slip was 4.53 in. (115 mm) before the spigot projection became engaged with the locking ring. The pipe reached a maximum axial force of 115 kips (516 kN) at 4.58 in. (116 mm) of joint displacement. Forces generated between the spigot projection and locking ring sheared the spigot projection off, allowing the spigot to slip out of the bell immediately after the peak load was reached.

Pipeline Response to Fault Rupture

A 40-ft (11.9-m)-long, seven-piece section of a ductile pipeline was tested at the Cornell Large-Scale Lifelines Facility. The pipe had six joints; three at 5, 15, and 18 ft (1.5, 4.6, and 5.5 m) north and three at the same distances south from a 50º fault. The pipeline was pressurized to approximately 80 psi (552 kPa). The pipe was placed on a bed of compacted partially saturated sand, aligned, instruments checked, and then backfilled with compacted sand to a depth of cover of 30 in. (0.76m) above the pipe crown. The test basin's north section was displaced along a 50º fault at a rate of 4.8 in. (122 mm) per minute. At a fault displacement of 44.4 in. (1130 mm), the pipe lost pressure, and the test was stopped. The 44.4 in. (1130 mm) fault displacement

corresponds to 28.5 in. (725 mm) of axial extension of the test basin and pipe. Following excavation, a fracture was observed at the west springline of the spigot projection of the S5 joint.

The test measurements confirm that the pipeline was able to accommodate successfully fault rupture through axial displacements and rotations at all six joints. Moreover, the measurements provide a comprehensive and detailed understanding of how the movement was accommodated at each joint, the sequence of movements, and combined axial pullout and rotation at each joint. The combined joint pullout displacements are 28.5 in. (725 mm), which exceeds the sum of the 4.5 in. (114 mm) spigot insertion length for all six joints. On average, the spigot at each joint pulled from the bell on the order of 4.75 in. (121 mm), thus showing that additional pullout occurs beyond the slip required for the spigot projection to make contact with the locking ring. The maximum rotation measured at the joints closest to the fault was about 8.5 degrees.

Significance of Test Results

Large-scale fault rupture tests at Cornell demonstrate the ability of the Kubota ERDIP joints to accommodate significant fault movement through axial pullout and rotation of the joints. Fault rupture simulated in the large-scale test is also representative of the most severe ground deformation that occurs along the margins of liquefaction-induced lateral spreads and landslides.

The amount of tensile strain that can be accommodated with the Kubota earthquake resistant ductile iron pipelines will depend on the spacing of the pipeline joints. The pipeline used in the large-scale split-basin test was able to accommodate 28.5 in. (725 mm) of axial extension, corresponding to an average tensile strain of 5.9% along the pipeline. Such extension is large enough to accommodate the great majority (over 99%) of liquefaction-induced lateral ground strains measured by high resolution LiDAR after each of four major earthquakes during the recent Canterbury Earthquake Sequence (CES) in Christchurch, NZ (O'Rourke, et al., 2014).. These high resolution LiDAR measurements for the first time provide a comprehensive basis for quantifying the ground strains caused by liquefaction on a regional basis. To put the CES ground strains in perspective, the levels of liquefaction-induced ground deformation measured in Christchurch exceed those documented in San Francisco during the 1989 Loma Prieta earthquake and in the San Fernando Valley during the 1994 Northridge earthquake. They are comparable to the levels of most severe liquefaction-induced ground deformation documented for the 1906 San Francisco earthquake, which caused extensive damage to the San Francisco water distribution system. The

tests confirm that the Kubota ERDIP joints are able to sustain without leakage large levels of ground deformation, the magnitude of which will vary depending on the ground deformation patterns and spacing of the joints.

TABLE OF CONTENTS

LIST OF FIGURES

LIST OF FIGURES (completed)

LIST OF TABLES

Section 1
Introduction and Organization

This report presents results from testing performed at Cornell University for 6-in. (150-mm)-diameter earthquake resistant ductile iron pipe (ERDIP) manufactured by the by Kubota Corporation. The purpose of the testing was to characterize the mechanical behavior of the earthquake-resistant ductile iron jointed pipe under direct tension and large-scale testing of fault rupture effects. The report is organized in four sections, the first of which provides introductory remarks and describes the report organization. Section 2 presents the results of a direct tension test performed to evaluate the axial force vs. displacement characteristics and associated leakage thresholds for this type of loading. Section 3 presents the results of fault rupture effects on a pipeline performed in the large-scale test basin at the Cornell University Large Scale Lifelines Testing Facility. Section 4 provides summary remarks and draws conclusions for the testing. It should be noted that the term "rotation" in this report is equivalent to "deflection" as used commonly in the field and commercial pipeline information.

Section 2
Joint Tension Test

2.1 Introduction

This report section summarizes the results of the tension testing of the Kubota earthquake resistant ductile iron pipe (ERDIP), referred to as GENEX in Japan. The bell has a rubber gasket to prevent leakage and is equipped with a locking ring. The spigot is inserted into the bell past the rubber gasket and the locking ring. The spigot has a special feature called a spigot projection that can bear against the locking ring, acting as a locking mechanism, when the joint is pulled. A schematic of the ERDIP joint is shown in Figure 2.1. The pipe joint specimen was 13.9-ft. (4.24 m)-long with an outside diameter of 6.65 in. (168.9 mm) and a wall thickness of 0.34 in. (8.64 mm.). The pipe was placed in the load frame so that the gap in the locking ring was located at the crown, as shown in Figure 2.2. The pipe was fully inserted into the bell at the beginning of the test. Fully inserted refers to the position when the end of the spigot was in contact with the base of the bell socket. Figure 2.3 provides a schematic of the tension test.

2.2 Instrumentation

Four strain gages were mounted 39 in. (991 mm) north of the bell face on the bell side of the pipe at the positions of 12, 3, 6, and 9 o´clock (crown, east springline, invert, and west springline, respectively). The other four strain gages were mounted 34 in. (864 mm) south of the bell face on the spigot side at the same positions. Four string pots, mounted on the bell at quarter points around the pipe circumference 12 in. (305 mm) from the bell face, were fixed to the spigot and used to measure axial pullout of the spigot from the bell. An actuator and a load cell were installed on the load frame to apply and measure tensile force at the end of the pipe. The instrument locations and gage names are listed in Table 2.1.

2.3 Force – Displacement

The pipe was filled with water and pressurized. The pressurizing sequence is shown in Figure 2.4. As the pressure was increased to 9 psi (62 kPa), there was a very small pullout movement of the spigot. The pressure was raised, lowered, and then raised slowly until the joint opened to 4.53 in. (115 mm) at a pressure of 30 psi (207 kPa). The pressure was then raised to 84 psi (579 kPa) in preparation for axial loading. The load applied in this test was calculated using the average

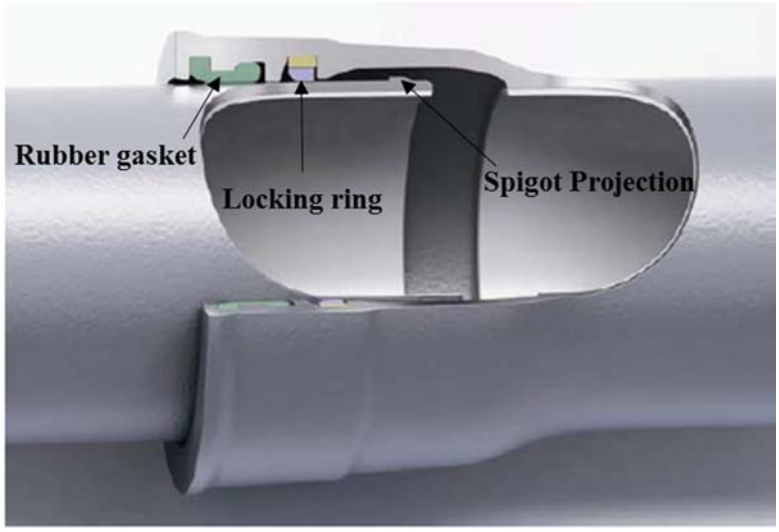

Figure 2.1. Cut-Away View of ERDIP GENEX Joint (courtesy Kubota Corp.)

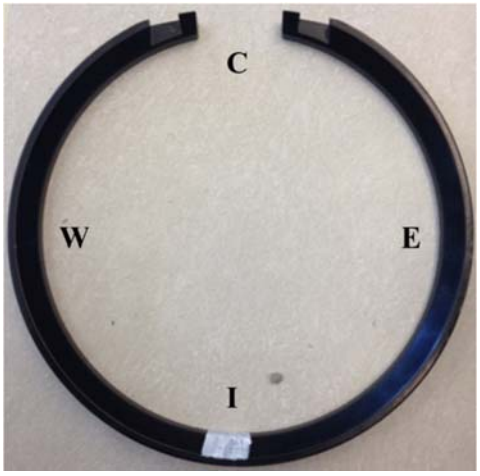

Figure 2.2. Locking Ring Orientation (Looking North)

strain gage measurements on both the bell and spigot segments. The two strain gage loads were within 2% of each other, and provide a reliable and consistent basis for axial force assessment. The load, P, was calculated as follows

$$P = \varepsilon EA \tag{2.1}$$

where ε is the average measured axial strain on each of the spigot and bell sides of the test specimen and E is Young's modulus for ductile iron of 24,700 ksi (170 GPa) based on ductile iron tensile coupon tests performed at Cornell University and provided by Kubota. The cross-sectional area, A, of the specimen was 6.74 in^2 (4348 mm^2).

Table 2.1. Instrumentation for Kubota ERDIP GENEX Joint Tension Test

Location	Instrument	Local Instrument Name
39 in. North of Bell Face	Crown, Axial Strain	B39C
39 in. North of Bell Face	Invert, Axial Strain	B39I
39 in. North of Bell Face	East Springline, Axial Strain	B39E
39 in. North of Bell Face	West Springline, Axial Strain	B39W
34 in South of Bell Face	Crown, Axial Strain	S34C
34 in South of Bell Face	Invert, Axial Strain	S34I
34 in South of Bell Face	East Springline, Axial Strain	S34E
34 in South of Bell Face	West Springline, Axial Strain	S34W
34 in South of Bell Face	Crown, Circumferential Strain	S34CC
34 in South of Bell Face	Invert, Circumferential Strain	S34IC
34 in South of Bell Face	East Springline, Circumferential Strain	S34EC
34 in South of Bell Face	West Springline, Circumferential Strain	S34WC
Bell Face	Crown String Pot	Jnt Opening C
Bell Face	Invert String Pot	Jnt Opening I
Bell Face	East Springline String Pot	Jnt Opening E
Bell Face	West Springline String Pot	Jnt Opening W
Actuator	Load Cell	PX302-10KV
Actuator	Displacement	Act Disp

1 in. = 25.4 mm

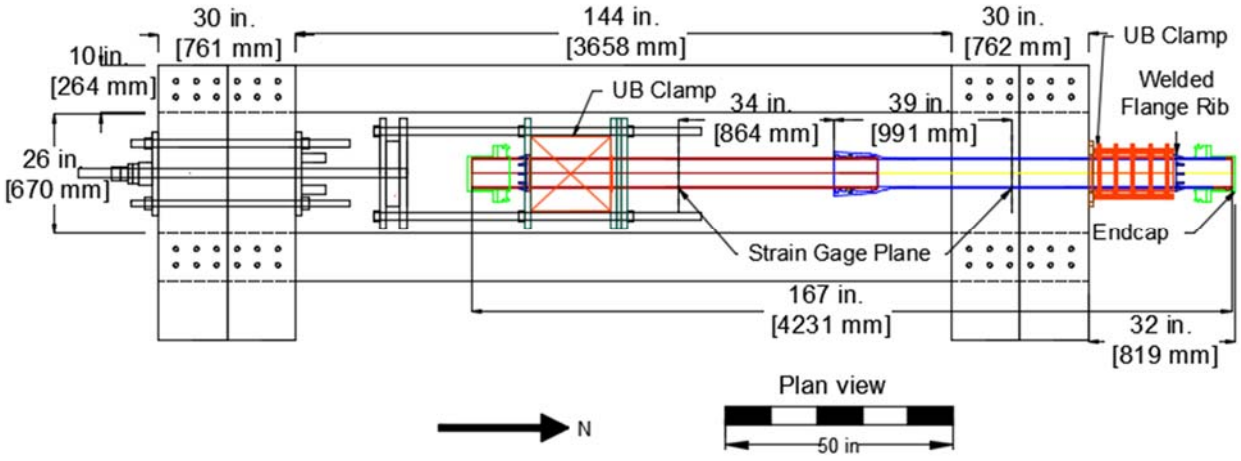

Figure 2.3. Tension Test Layout

The load, P, is the axial tensile force plotted in Figures 2.5 and 2.6. The axial force also was measured by the load cell after the pipe was pressurized. The sum of the maximum load cell measurement and axial force generated by internal pressure on the end caps was 117 kips, which agrees well with the average strain gage axial load measurements (within 2 %).

The pipe was secured to the actuator, and loading began at a rate of 0.72 in. (18 mm) per minute. Figures 2.5 and 2.6 show the tensile force plotted against actuator displacement and average joint opening, respectively. A peak load of 115 kips (516 kN) was attained at 0.47 in. (12 mm) of actuator displacement and 4.58 in. (116 mm) of joint opening. This force exceeds the manufacturer's estimated maximum tensile force of 3.0D, where D is the nominal diameter in mm and the force is expressed in kN to give approximately 101 kips (450 kN).

As tensile force was applied, the spigot was pulled from the bell, thus causing the spigot projection to bear against the locking ring. As the tensile force increased, the load carried by the locking ring also increased. When the pipe reached the maximum load, part of spigot projection was sheared from the spigot. The spigot was pulled from the bell immediately after the peak load, resulting in leakage. Leakage was not observed before peak load.

2.4 Spigot Deformations

The diameter of the spigot was measured at four different locations: Crown to Invert (C to I), Crown East to Invert West (CE to IW), East to West (E to W) and Invert East to Crown West (IE to CW) as shown in Figure 2.7. The outer diameter of the spigot was measured before the tension test. The measurements showed that the spigot had a circular cross-section with an average diameter of 6.64 in. (169 mm) along its length.

Diameter measurements after the test were taken at 5 different locations along the length of the spigot at 0.5 in. (12.7 mm) (spigot end), 1 in. (25.4 mm) (front of spigot projection), 1.5 in. (38.1 mm) (behind spigot projection), and 3 in. (76.2 mm). The diameter measurements are presented in Table 2.2. The range of the spigot diameters at the four locations shown in Figure 2.7 is between 6.62 in. (168 mm) and 6.65 in. (169 mm) within 3 in. (76.2 mm) from the end of the spigot. Spigot ovaling was not observed because the locking ring distributed the applied stress onto the spigot projection along the circumference of the spigot.

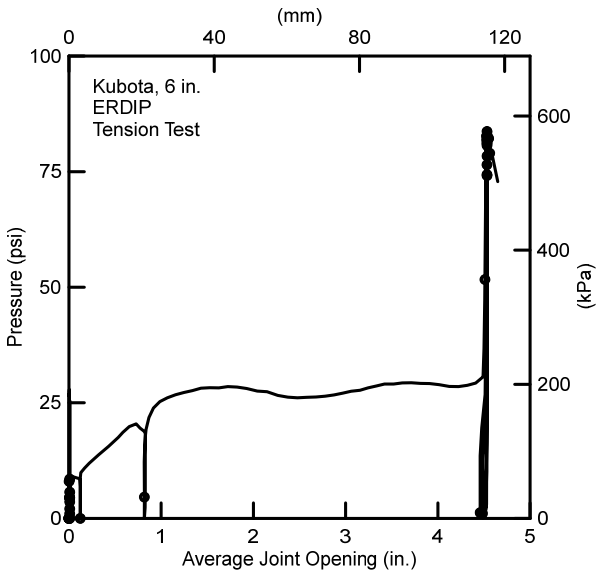

Figure 2.4. Pressure vs. Average Joint Opening

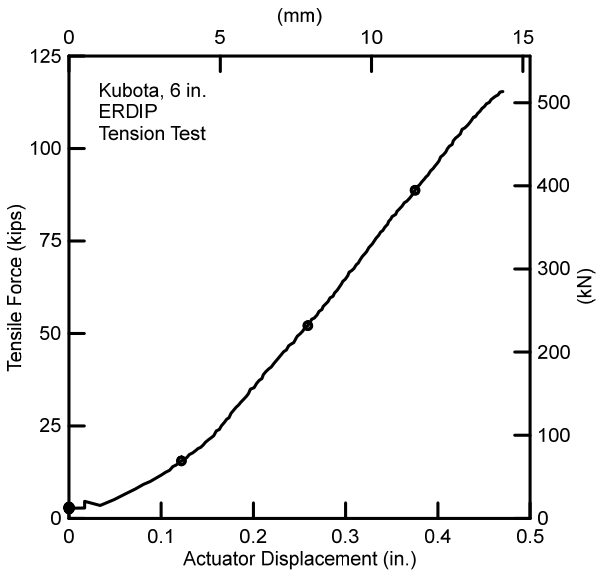

Figure 2.5. Tensile Force vs. Actuator Displacement

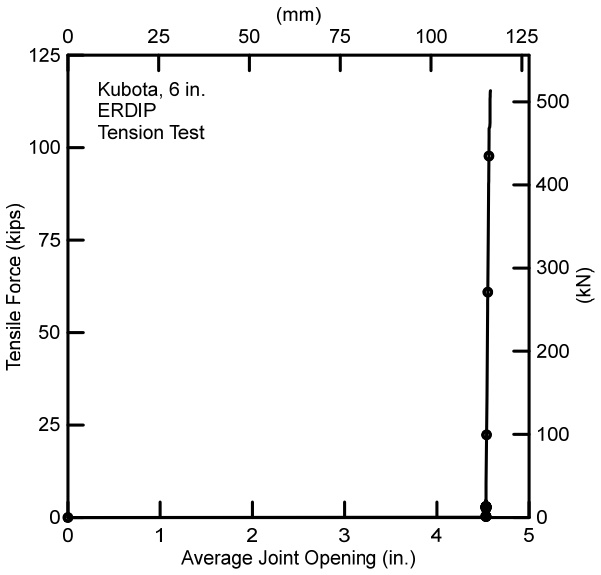

a) Full Range

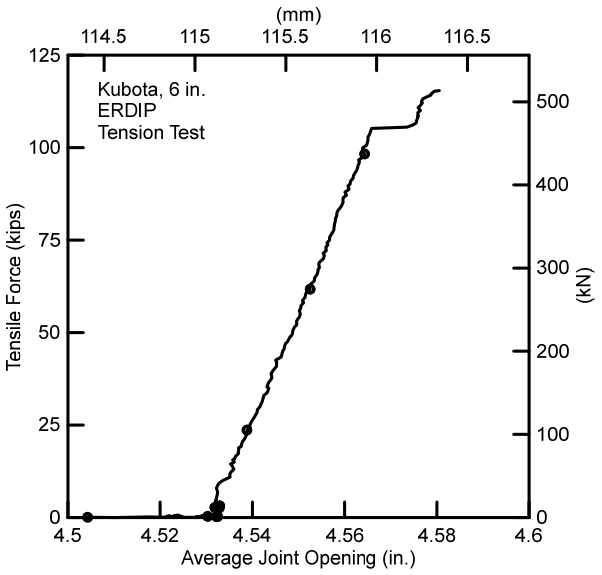

b) Between 4.5 and 4.6 in. (114.3 and 116.8 mm) of Joint Opening

Figure 2.6. Tensile Force vs. Average Joint Opening

Table 2.2. Diameter Measurements on Spigot Section

Pre-Test				
Locations	C-I (in.)	CE-IW (in.)	E-W (in.)	CW-IE (in.)
Spigot End	6.630	6.645	6.633	6.620
Post-Test				
Locations	C-I (in.)	CE-IW (in.)	E-W (in.)	CW-IE (in.)
0.5 in. from End	6.620	6.643	6.623	6.639
1 in. from End	6.620	6.633	6.632	6.644
1.5 in. from End	6.619	6.633	6.620	6.636
3 in. from End	6.625	6.639	6.627	6.648

1 in. = 25.4 mm

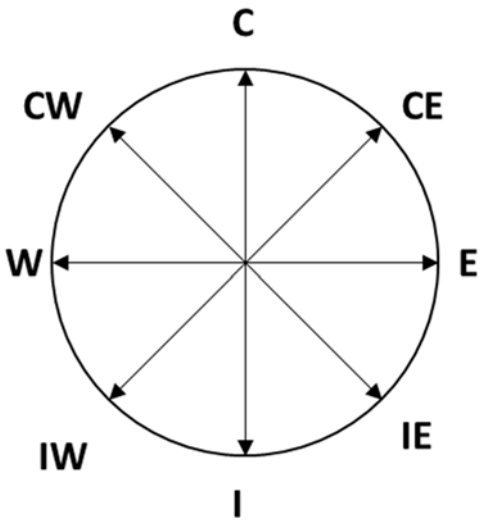

Figure 2.7. Spigot Measurement Locations (Looking North)

2.5 Spigot Axial Strains

The maximum axial tensile strain on the spigot side was 776 με (0.0776%) and developed at the invert at the maximum load of 115 kips (516 kN) at 0.47 in. (12 mm) of actuator displacement and 4.58 inches (116 mm) of joint opening. The relationships between spigot axial strains and the tensile force, actuator displacement, and joint opening are shown in Figures 2.8, 2.9, and 2.10, respectively. Recall that there was a rapid joint opening of roughly 4.53 in. (115 mm) as internal pressure was applied.

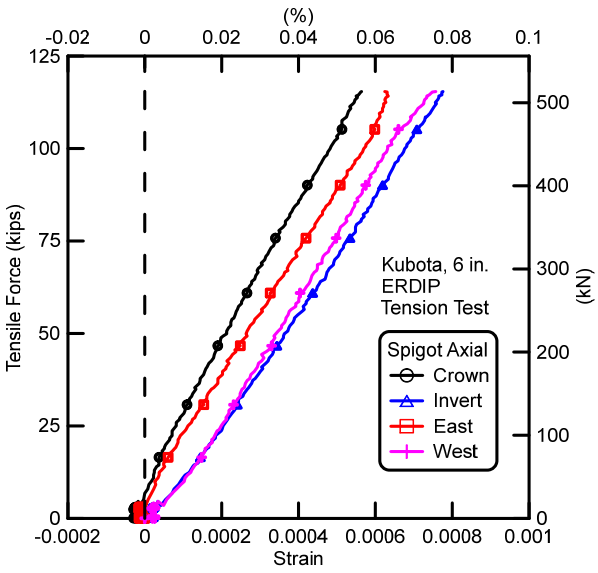

Figure 2.8. Tensile Force vs. Spigot Axial Strain

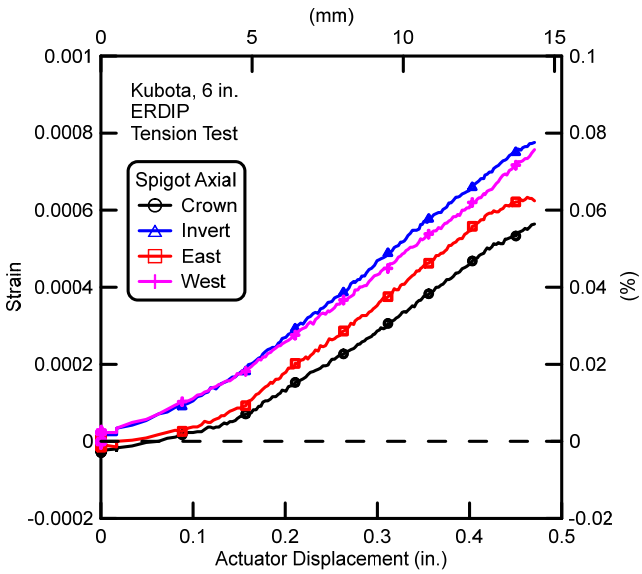

Figure 2.9. Spigot Axial Strain vs. Actuator Displacement

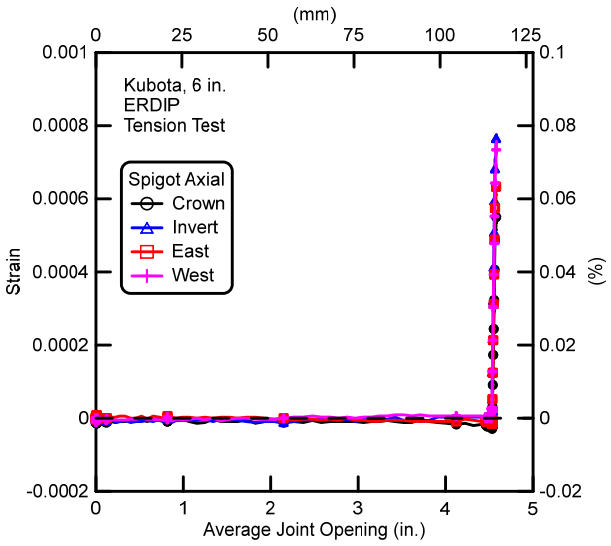

a) Full Range

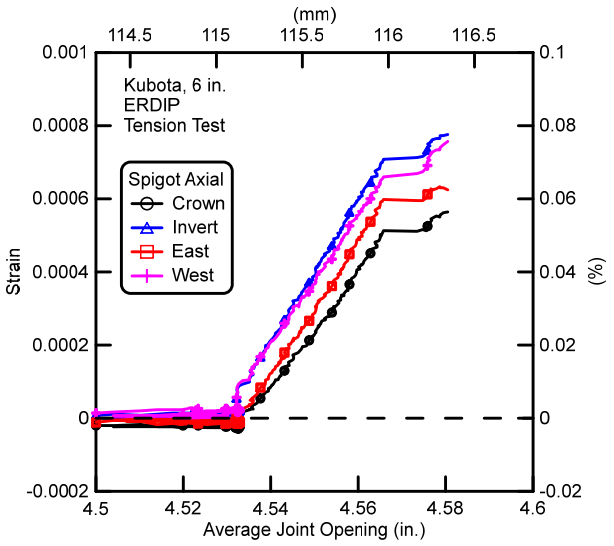

b) Between 4.5 and 4.6 in. (114.3 and 116.8 mm) of Joint Opening

Figure 2.10. Spigot Axial Strain vs. Average Joint Opening

As shown in Figures 2.8 and 2.9, the greatest difference in strain is between the crown and invert, indicating that the bending strain was larger in the crown-invert direction relative to the east-west springline direction. The gap in the locking ring was located at the crown (see Figure 2.1), thereby contributing to eccentric load distribution and associated moment.

2.6 Spigot Hoop Strains

Figures 2.11, 2.12, and 2.13 show the tensile force vs. the spigot hoop strain, the spigot hoop strain vs. the actuator displacement, and the spigot hoop strain vs. the average joint opening, respectively. Spigot hoop strains at four positions (crown, invert, east, and west) were all initially positive (tensile), caused by internal pressure. The actuator then started pulling the spigot. When the spigot projection made contact with the locking ring, compressive forces were developed at the contact between the locking ring and spigot, causing the spigot hoop strain to decrease and become negative (compressive). The maximum compressive hoop strain of 0.0002 (0.02%) was measured at the invert. Since the gap in the locking ring was located at the crown, the crown of the spigot experienced less compressive force than other locations. Consequently, the crown hoop strain was less than the invert, east, and west hoop strains.

2.7 Bell Axial Strains

The relationships between bell axial strains and the tensile force, actuator displacement, and joint opening are shown in Figures 2.14, 2.15, and 2.16, respectively. The maximum tensile axial strain measured in the bell was 1,140 με (0.114%) at the invert at the maximum load of 115 kips (516 kN) at 0.47 in. (12 mm) of actuator displacement and 4.58 inches (116 mm) of joint opening.

As shown in Figures 2.14 and 2.15, there is a substantial difference in strain between the crown and invert. This difference is larger than the strain difference shown in Figures 2.7 and 2.8 and is related to an increase in bending moment as eccentric loads are transferred from the spigot to the larger diameter bell.

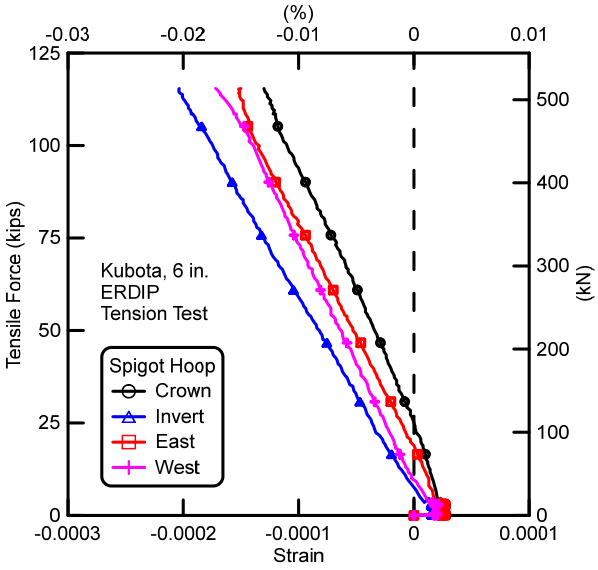

Figure 2.11. Tensile Force vs. Spigot Hoop Strain

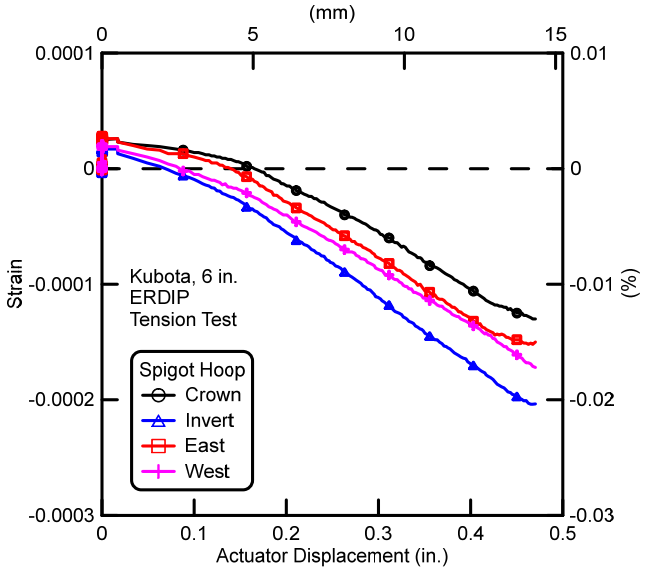

Figure 2.12. Spigot Hoop Strain vs. Actuator Displacement

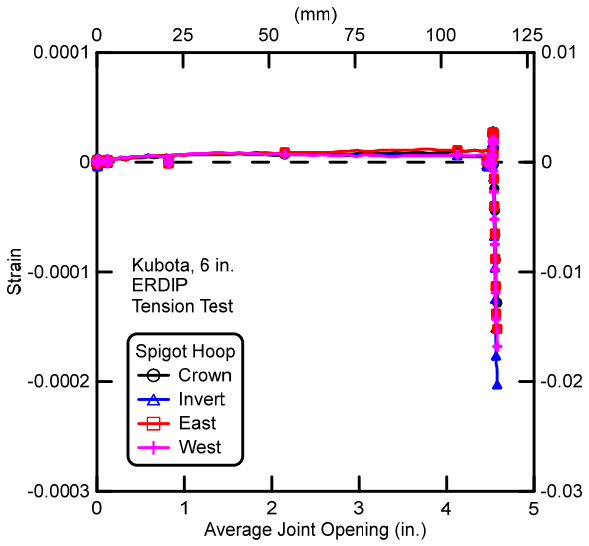

a) Full Range

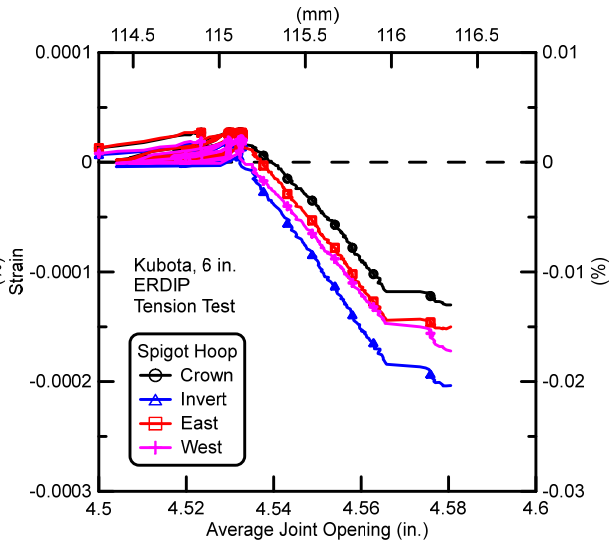

b) Between 4.5 and 4.6 in. (114.3 and 116.8 mm) of Joint Opening

Figure 2.13. Spigot Hoop Strain vs. Average Joint Displacement

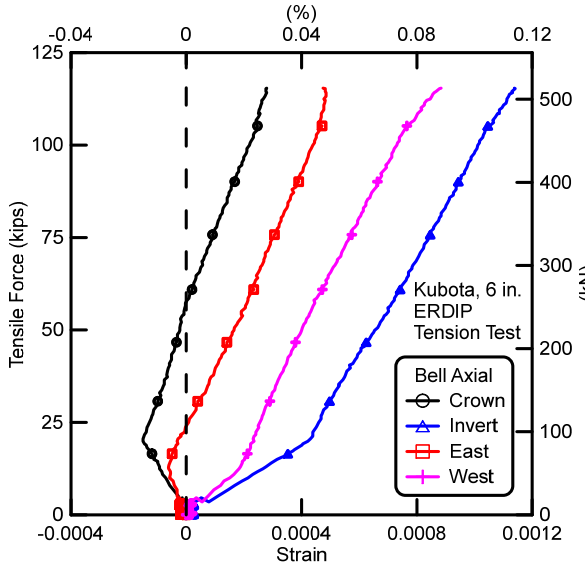

Figure 2.14. Tensile Force vs. Bell Axial Strain

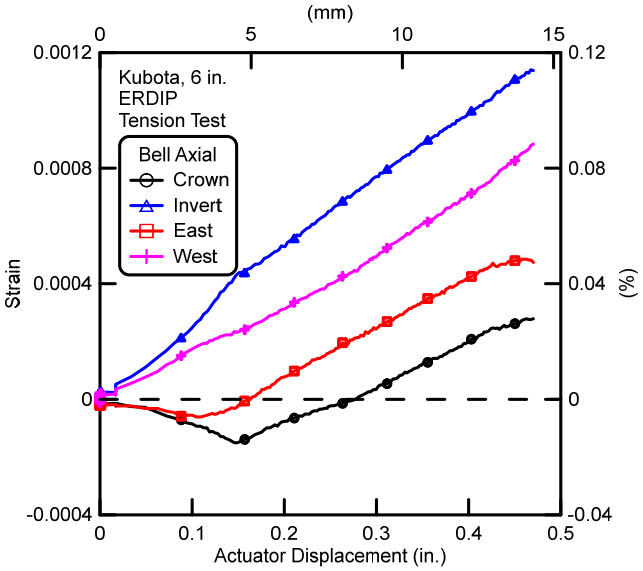

Figure 2.15. Bell Axial Strain vs. Actuator Displacement

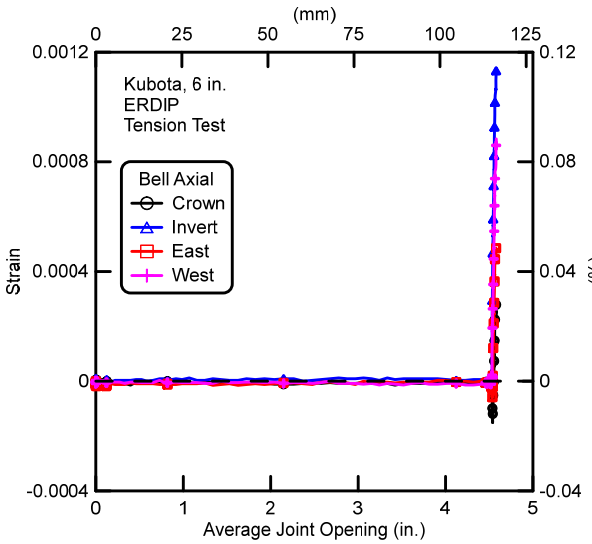

a) Full Range

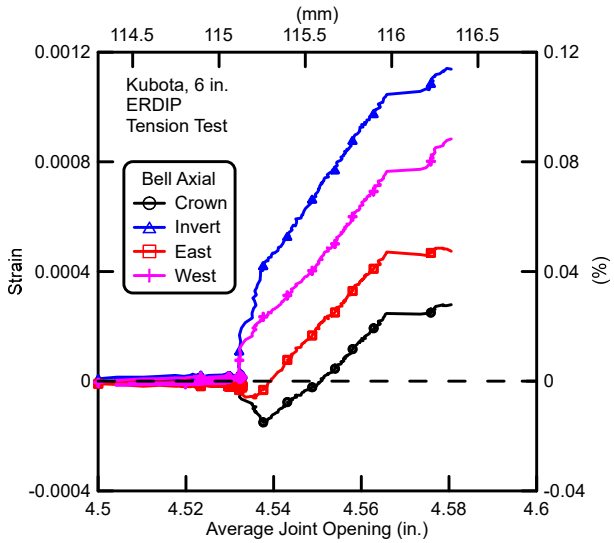

b) Between 4.5 and 4.6 in. (114.3 and 116.8 mm) of Joint Opening

Figure 2.16. Bell Axial Strain vs. Average Joint Opening

2.8 Conclusions

A joint tension test was performed on the 6-in. (150-mm)-diameter Kubota earthquake resistant ductile iron pipe (ERDIP). The test began with the spigot fully inserted in the bell. As the pipe was pressurized, the spigot was displaced from the bell seat at approximately 9 psi (62 kPa) internal pressure. The slip was 4.53 in. (115 mm) before the spigot projection became engaged with the locking ring. The pipe reached a maximum force of 115 kips (516 kN) at 4.58 in. (116 mm) of joint displacement. This force is higher than the manufacturer's maximum tensile force estimate of 101 kips (450 kN), given by 3.0 D where D in the nominal pipe diameter of 150 mm and the force is expressed in kN. Forces generated between the spigot projection and locking ring sheared the spigot projection off, allowing the spigot to slip out of the bell immediately after the peak load was reached and caused leakage. Leakage was not observed before peak load.

Section 3
Large-Scale Testing of Fault Rupture Effects

3.1 Introduction

This section presents the results of a large-scale test of fault rupture effects on a ductile iron pipeline, composed of earthquake resistant ductile iron pipe (ERDIP) provided by Kubota. All testing was performed in the large-scale test basin at the Cornell University Large Scale Lifelines Testing Facility during September 2015. It should be noted that the term "rotation" in this section is equivalent to "deflection" as used commonly in the field and commercial pipeline information.

3.2 Test Configuration and Procedure

Figure 3.1 is a plan view of the test layout, which shows the fault rupture plane and approximate locations of the four actuators generating ground failure. The pipeline consisted of seven pipe segments of Kubota ERDIP. The objective of the test was to impose abrupt ground deformation on the pipeline, which was representative of left lateral strike slip fault rupture and the most severe ground deformation that occurs along the margins of liquefaction-induced lateral spreads and landslides. The pipeline was constructed to evaluate its capacity to accommodate full-scale fault movement through the simultaneous axial pullout at six different joints. Measuring simultaneous performance of multiple joints allows for confirmation that the pipeline will respond to ground failure as intended, understand the complex interaction among the different joints, and determine the maximum ground deformation and axial pipeline load that can be sustained before joint leakage.

The pipeline was buried in the Cornell large-scale test basin in partially saturated sand that was compacted to have an average friction angle of 42º, equivalent in strength to that of a medium dense to dense granular backfill. The pipeline was assembled so that the spigot at each joint could pull from the bell approximately 4.5 in. (114 mm) before the spigot projection made contact with the locking ring. The depth of burial to top of pipe was 2.5 ft (0.76 m). During the test, the south part of the basin remained stationary, while the north part was displaced to the north and west by large-stroke actuators to cause soil rupture and slip at the interface between the two parts of the test basin.

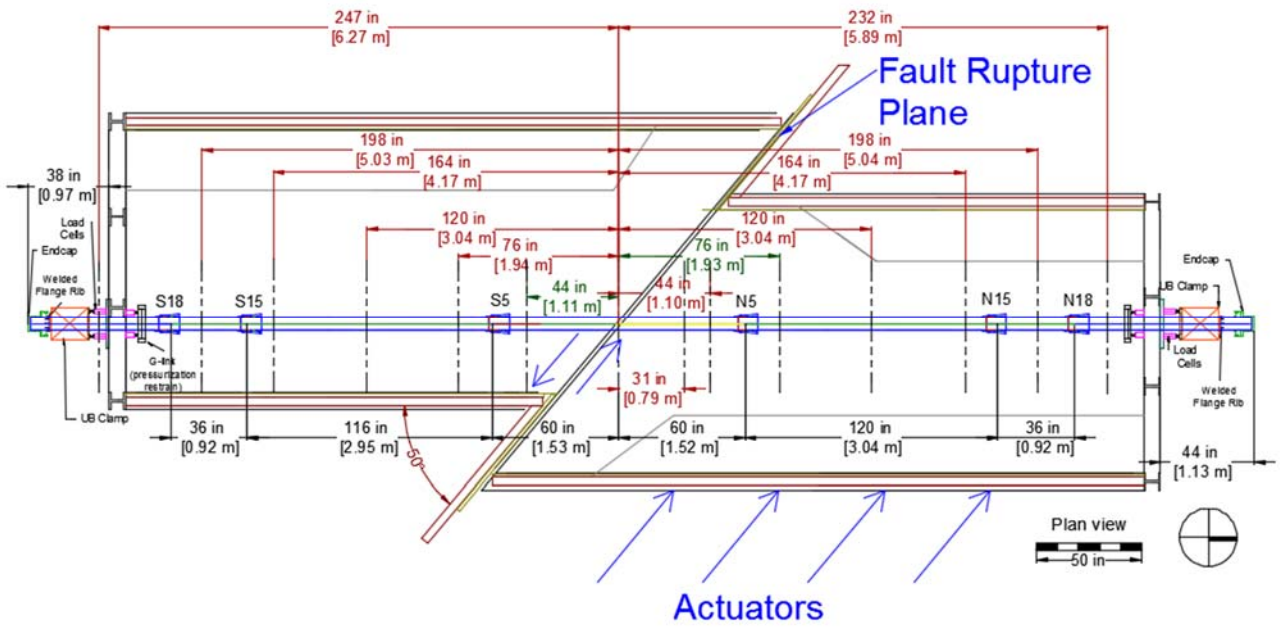

Figure 3.1. Plan View of Kubota ERDIP Pressurized Pipe Centered Specimen in Test Basin

A 128-in. (3.25-m)-long pipe section was placed directly over the fault, with an intersection angle of 50°. Two identical 128-in. (3.25 m)-long pipes were installed to the north and the south of the center pipe. Two 36-in. (0.91 m)-long pipes were assembled to the north and the south of the three identical 128-in. (3.25 m)-long pipes. An 87-in. (2.2-m)-long pipe was connected at the north end of the pipeline and had 36 in. (0.91 m) of its portion buried in the soil. Lastly, a 71-in. (1.8-m)-long pipe was connected at the south end of the pipeline with 25 in. (0.64 m) of its portion in the test basin. The length of the pipeline buried in soil, also described as the "test portion," was approximately 40 ft (12 m) long. The test basin was backfilled with compacted sand with a depth to pipe crown of 30 in. (0.76 m).

The pipe was pressurized with water to approximately 80 psi (552 kPa). The north (movable) portion of the test basin was connected to four MTS hydraulic actuators with load cells controlled by a MTS Flextest GT controller. All actuators were operated in synchronized displacement control. The general test procedure, after all soil placement and instrumentation were installed was:

a) Verify pipe internal pressure,

b) Move the test basin 1 in. (25.4 mm) at a rate of 4.8 in./minute (122 mm/minute),

c) Verify data collection, and system integrity

e) Begin moving basin again until pipe failure.

The simulated fault rupture caused both tensile and bending strains in the pipeline. At a fault displacement of 44.4 in. (1130 mm), the internal pressure dropped to 25 psi (172 kPa), indicating leakage in the pipeline. The test was then stopped. No leakage was observed until the fault displacement reached 44.4 in. (1130 mm).

3.3 Instrumentation

Figure 3.1, a plan view of the test layout, shows the locations of the instruments along the test pipeline. The instrumentation consisted of strain gages at fourteen locations (gage planes) along the pipeline, load cells at the ends of the pipeline and string pots to measure joint displacements. Sixty-four strain gages were installed in fourteen locations along the pipeline to measure strains and to evaluate axial forces and bending moments. Strain gages were positioned at the crown (C) and invert (I), and at the east (E) and west (W) springlines of the pipe. Table 3.1 provides the number of strain gage station locations with respect to the fault and joints. Strain gage locations were chosen on the basis of the expected deformed shape and axial behavior of the pipeline as determined from axial pull tests performed at Cornell University as well as the results of finite element analyses of the test. Strain gage stations S247 and S232 were intended to provide measurements of the end loads. Strain gage stations close to the joints, S198 S164, S76, N76, N164, and N198, were placed to assess strain concentration near the joints. Table 3.1 provides locations and coding for the fourteen gage planes.

Figure 3.2 shows the setup of the string pots. Three string pots were placed at each joint to measure the joint pullout and rotation, as well as spigot to bell face relative movement. Table 3.2 provides the locations and the labeling of the joint string pots to measure joint pullout and rotation. Two string pots were mounted at the east and west springlines of the bell. The other string pot was installed at the crown of the bell.

Table 3.1. Strain Gage Locations and Coding System for Kubota Pressurized ERDIP Test

Gage Station	Gages	Distance from Fault	Distance from Closest Joint Bell Face
S247	S247E-East Springline, Longitudinal S247C-Crown, Longitudinal S247W-West Springline, Longitudinal S247I-Invert, Longitudinal	247 in. (6.27 m) south	38 in. (0.97 m) south of the S18 joint
S198	S198E-East Springline, Longitudinal S198C-Crown, Longitudinal S198W-West Springline, Longitudinal S198I-Invert, Longitudinal	198 in. (5.03 m) south	11 in. (0.27 m) north of the S18 joint
S164	S164E-East Springline, Longitudinal S164C-Crown, Longitudinal S164W-West Springline, Longitudinal S164I-Invert, Longitudinal	164 in. (4.17 m) south	6 in. (0.11 m) north of the S15 joint
S120	S120E-East Springline, Longitudinal S120C-Crown, Longitudinal S120W-West Springline, Longitudinal S120I-Invert, Longitudinal	120 in. (3.04 m) south	50 in. (1.27 m) north of the S15 joint
S76	S76E-East Springline, Longitudinal S76C-Crown, Longitudinal S76W-West Springline, Longitudinal S76I-Invert, Longitudinal	76 in. (1.94 m) south	25 in. (0.62 m) south of the S5 joint
S44	S44EA-East Springline, Longitudinal S44CA-Crown, Longitudinal S44WA-West Springline, Longitudinal S44IA-Invert, Longitudinal S44EC-East Springline, Circumferential S44CC-Crown, Circumferential S44WC-West Springline, Circumferential S44IC-Invert, Circumferential	44 in. (1.11 m) south	8 in. (0.21 m) north of the S5 joint
0	0E-East Springline, Longitudinal 0C-Crown, Longitudinal 0W-West Springline, Longitudinal 0I-Invert, Longitudinal	0	52 in. (1.32 m) south of the north joint
N31	N31E-East Springline, Longitudinal N31C-Crown, Longitudinal N31W-West Springline, Longitudinal N31I-Invert, Longitudinal	31 in. (0.79 m) north	35 in. (0.89 m) south of the N5 joint
N44	N44E-East Springline, Longitudinal N44C-Crown, Longitudinal N44W-West Springline, Longitudinal N44I-Invert, Longitudinal	44 in. (1.1 m) north	23 in. (0.57 m) south of the N5 joint

Table 3.1. Strain Gage Locations and Coding System for Kubota Pressurized ERDIP Test (Completed)

Gage Station	Gages	Distance from Fault	Distance from Closest Joint Bell Face
N76	N76EA-East Springline, Longitudinal N76CA-Crown, Longitudinal N76WA-West Springline, Longitudinal N76IA-Invert, Longitudinal N76EC-East Springline, Circumferential N76CC-Crown, Circumferential N76WC-West Springline, Circumferential N76IC-Invert, Circumferential	76 in. (1.93 m) north	10 in. (0.26 m) south of the N5 joint
N120	N120E-East Springline, Longitudinal N120C-Crown, Longitudinal N120W-West Springline, Longitudinal N120I-Invert, Longitudinal	120 in. (3.04 m) north	54 in. (1.37 m) north of the N5 joint
N164	N164E-East Springline, Longitudinal N164C-Crown, Longitudinal N164W-West Springline, Longitudinal N164I-Invert, Longitudinal	164 in. (4.17 m) north	20 in. (0.5 m) south of the N15 joint
N198	N198E-East Springline, Longitudinal N198C-Crown, Longitudinal N198W-West Springline, Longitudinal N198I-Invert, Longitudinal	198 in. (5.04 m) north	15 in. (0.37 m) north of the N15 joint
N232	N232E-East Springline, Longitudinal N232C-Crown, Longitudinal N232W-West Springline, Longitudinal N232I-Invert, Longitudinal	232 in. (5.89 m) north	9 in. (0.23 m) north of the N18 joint

The spigot was inserted into the bell at each joint approximately 4.5 in. (114 mm). After the instrumentation was installed, protective shielding was wrapped around the joint. Figure 3.3 is an overview of the pipe joint with the protective shielding. Eight calibrated load cells were positioned at the ends of the test basin. Table 3.3 provides the locations and the labeling of the load cells.

Table 3.2. String Pot Locations and Labeling for Kubota Pressurized ERDIP Test

Location	Displacement Measurement Device	Type and Stroke
S18 Joint	S18 Disp E – East Springline S18 Disp C – Crown S18 Disp W – West Springline	String pot ± 10 in. String pot ± 10 in. String pot ± 10 in.
S15 Joint	S15 Disp E – East Springline S15 Disp C – Crown S15 Disp W – West Springline	String pot ± 10 in. String pot ± 10 in. String pot ± 10 in.
S5 Joint	S5 Disp E – East Springline S5 Disp C – Crown S5 Disp W – West Springline	String pot ± 10 in. String pot ± 10 in. String pot ± 10 in.
N5 Joint	N5 Disp E – East Springline N5 Disp C – Crown N5 Disp W – West Springline	String pot ± 10 in. String pot ± 10 in. String pot ± 10 in.
N15 Joint	N15 Disp E – East Springline N15 Disp C – Crown N15 Disp W – West Springline	String pot ± 10 in. String pot ± 10 in. String pot ± 10 in.
N18 Joint	N18 Disp E – East Springline N18 Disp C – Crown N18 Disp W – West Springline	String pot ± 10 in. String pot ± 10 in. String pot ± 10 in.

1 in. = 25.4 mm

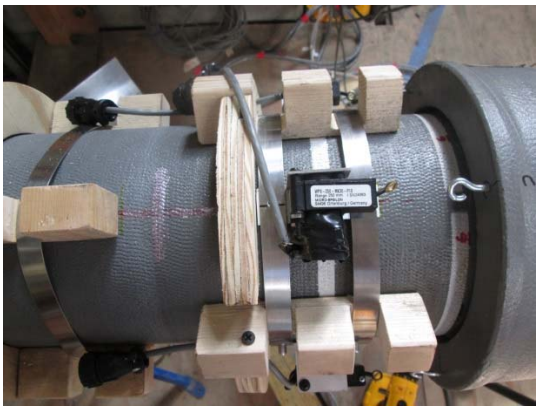

Figure 3.2 Setup of String Pots

Figure 3.3. Pipe Joint with Protective Shielding

Table 3.3. Load Cell Locations and Labeling for Kubota Pressurized ERDIP Test

Location	Load Cell
South End	SW Top Ld – Outer, West, Top SE Top Ld – Outer, East, Top SW Bot Ld – Outer, West, Bottom SE Bot Ld – Outer, East, Bottom
North End	NW Top Ld – Outer, West, Top NE Top Ld – Outer, East, Top NW Bot Ld – Outer, West, Bottom NE Bot Ld – Outer, East, Bottom

3.4 Soil Preparation and Compaction Data

The soil used during the test was crushed, washed, glacio-fluvial sand produced by RMS Gravel consisting of particles mostly passing the ¼ in. (6.35 mm) sieve. Figure 7.4 is the grain size distribution of the RMS graded sand. Eight inches (203 mm) of compacted sand was placed in the test basin, followed by the pipe sections, followed by approximately 8-in. (203-mm)-thick lifts until there was 30 in. (0.76 m) cover of compacted sand above the pipe crown. Every layer was compacted to the same extent and moistened with water in a similar way to achieve uniformity. Dry density measurements were taken for each layer using a Troxler Model 3440 densitometer. Moisture content measurements were obtained using both soil samples and the densitometer at the same locations. The target value of dry density was γ_{dry} = 106 lb/ft^3 (16.7 kN/m^3) and the target value of moisture content was w = 4.0 %, corresponding to an angle of shearing resistance (friction angle) of the sand of approximately 42º.

Eight measurements of dry unit weight and moisture content were made for each soil lift. Figure 3.5 shows the approximate location of each measurement location. There were four measurement positions in the north portion of the test basin and four in the south portion. Table 3.4 lists the dry unit weights. Table 3.5 provides the moisture contents. The global average dry unit weight was 105.6 lb/ft^3 (16.6 kN/m^3) with a standard deviation of 1.5 lb/ft^3 (0.24 kN/m^3). The global average moisture content was 3.7% with a standard deviation of 0.5%.

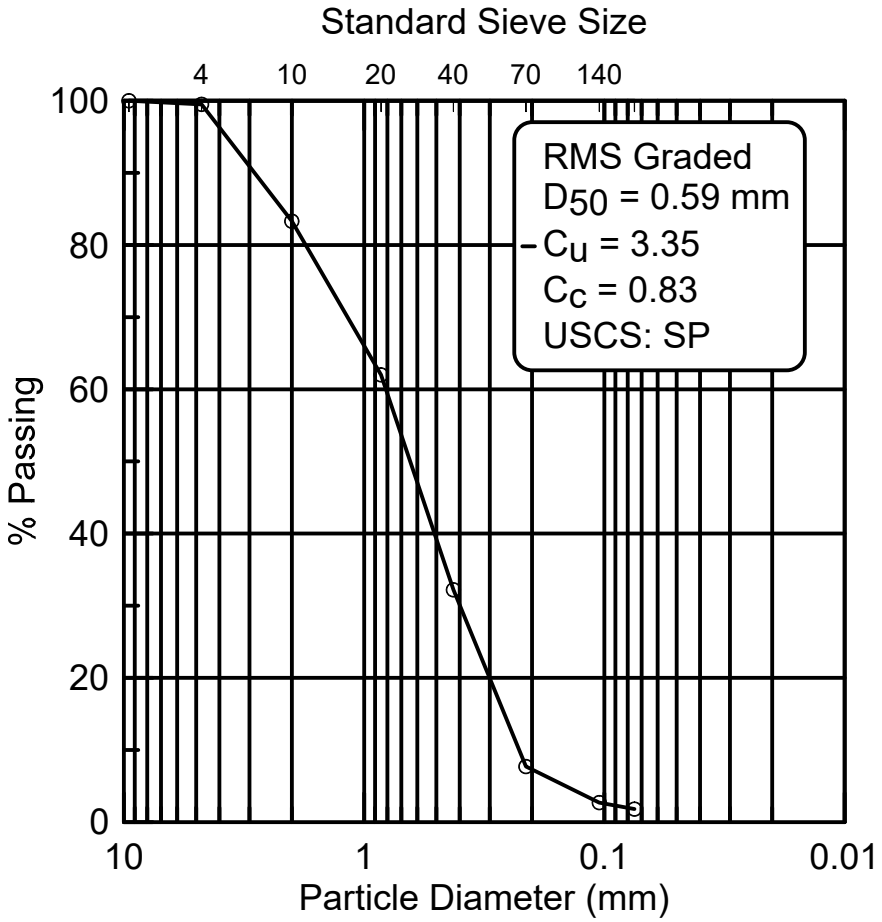

Figure 3.4. Particle Size Distribution of RMS Graded Sand

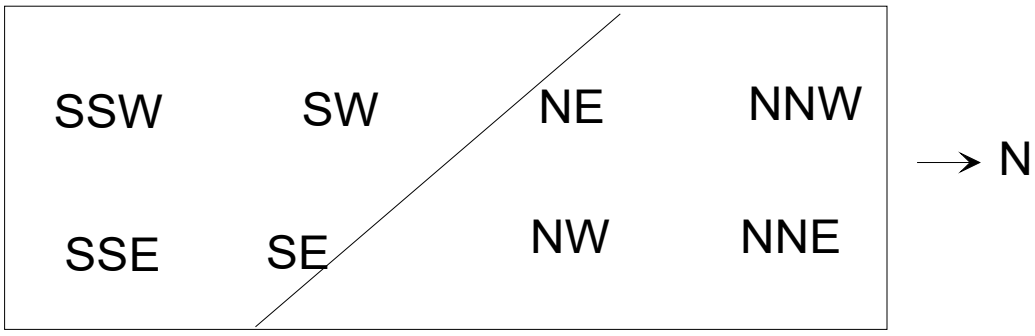

Figure 3.5. Plan View of Locations for Compaction Measurements

Table 3.4. Dry Unit Weights for Kubota Pressurized ERDIP Test

	Dry Unit Weights (lb/ft^3)[a]				
Location	Lift 1	Lift 2	Lift 3	Lift 4	Lift 5
NNW	105.6	105.6	106.8	105.7	107.3
NW	105.7	106.1	104.3	104.7	105.8
SSW	103.8	104.2	106.0	105.5	106.0
SW	105.2	108.2	103.1	104.1	104.4
SE	106.1	104.9	106.7	103.3	108.3
SSE	103.4	103.7	106.2	106.2	106.3
NE	107.6	104.2	105.8	106.8	108
NNE	103.6	103.4	106.8	105.2	107.8
Average	105.1	105.0	105.7	105.2	106.7
Stdev	1.4	1.6	1.4	1.1	1.4
Global Average					105.6
Global Stdev					1.5

1 (lb/ft^3) = 0.1571 kN/m^3

Table 3.5. Moisture Tin Water Content Data for Kubota Pressurized ERDIP Test

	Moisture Tin Water Content, w (%)				
Location	Lift 1	Lift 2	Lift 3	Lift 4	Lift 5
NNW	3.6	3.2	3.1	3.7	3.6
NW	4.4	3.6	3.5	4.3	3.7
SSW	4.2	4.8	3.8	3.7	3.2
SW	4.1	4.0	3.6	4.6	2.9
SE	4.2	4.6	3.7	4.0	3.6
SSE	3.8	4.8	4.2	3.9	3.8
NE	3.1	3.2	2.6	3.6	3.5
NNE	4.6	3.3	2.7	3.5	3.4
Average	4.0	3.9	3.4	3.9	3.5
Stdev	0.5	0.7	0.6	0.4	0.3
Global Average					3.7
Global Stdev.					0.5

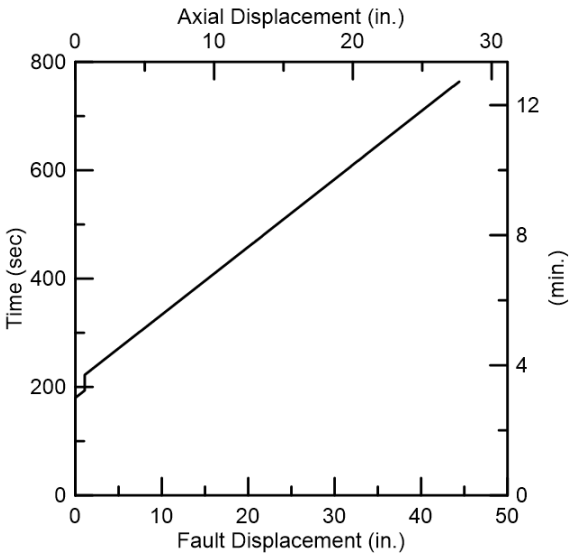

Figure 3.6 Fault Displacement vs. Time

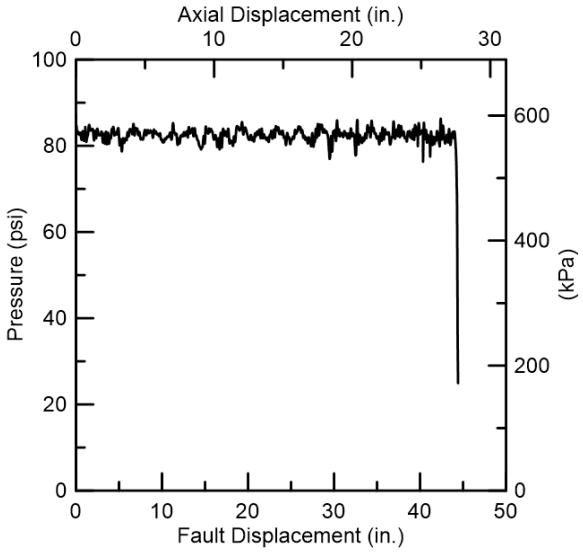

Figure 3.7. Internal Pipe Pressure vs. Fault Displacement

The angle of shearing resistance of the soil, based on correlations with soil unit weight established at Cornell, was 41-42°. The soil strength properties are representative of a well-compacted dense sand.

3.5 Test Basin Movements

Four actuators are connected between the movable portion of the test basin and the modular reaction wall in the laboratory. From south to north, the actuators are called short-stroke actuator 1 (SSA1), short-stroke actuator 2 (SSA2), long-stroke actuator 1 (LSA1), and long-stroke actuator 2. (LSA2). Each SSA actuator has a displacement range of ± 2 ft (± 0.61 m) for a total stroke of 4 ft (1.22 m) and load capacity of 100 kips (445 kN) tension and 145 kips (645 kN) compression. Each LSA actuator has a displacement range of ± 3 ft (0.91 m) for a total stroke of 6 ft (1.83 m) and load capacity of 63 kips (280 kN) tension and 110 kips (489 kN) compression.

Figure 3.6 shows the average displacement of the four actuators, which equals the fault displacement, with respect to time. The axial displacement imposed on the pipeline by fault displacement, d_f, is shown along the top horizontal axis. It is equal to $d_f \cos\beta$, for which β is the angle of intersection between the pipeline and the fault.

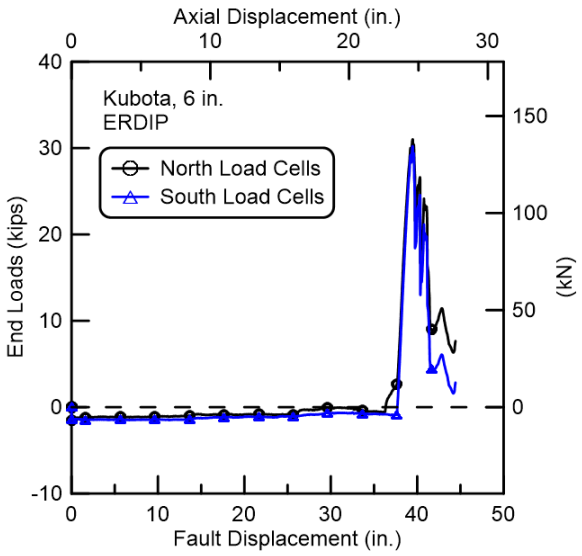

Figure 3.8 South and North Load Cells vs. Fault Displacement

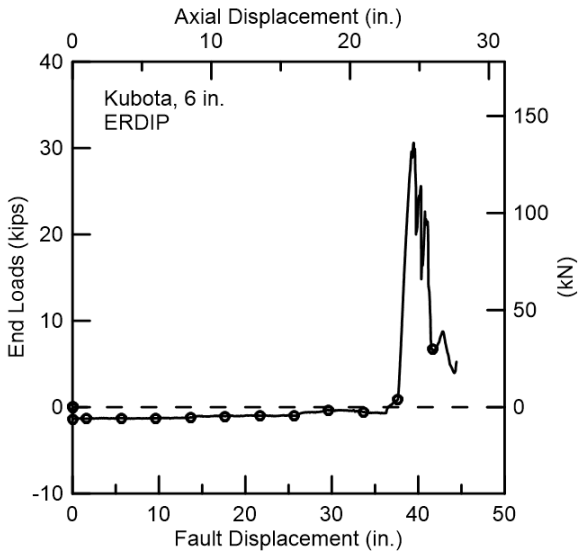

Figure 3.9 Average End Loads vs. Fault Displacement

3.6 Pipe Internal Pressure

The pipe was initially pressurized to 82 psi (565 kPa) before any basin movement and provided constant pressure during the test from the laboratory water supply. Each movement of the basin caused the pipe to increase slightly in overall length, causing moderate fluctuations in pressure. Figure 3.7 shows the pipe internal pressure vs. fault displacement. At a fault displacement of roughly 44.4 in. (1.13 m) there was a large loss of pressure in the pipe. This fault displacement corresponds to 28.5 in. (0.724 m) of axial pipeline displacement. At this point the test was stopped and the water drained from the pipe.

3.7 End Loads and Axial Forces

The end tensile loads were measured with four load cells at the south end of the test basin and four load cells at the north end. The sum of the four load cells at each end gives the total load at that end. Figure 3.8 shows the total load at the south and north ends of the test basin vs. fault displacement. The initial reduction of approximately 1 kip (4 kN) in the end loads was caused by internal pressurization. The loads at both ends did not exceed the initial load reduction at the first 36 in. (914 mm) of fault displacement. The loads at the north end sharply increase at a fault displacement of approximately 36.3 in. (922 mm), but the loads at the north end did not begin to increase until a fault displacement of 37.5 in. (953 mm). Thus, there was about 1.2 in. (30.5 mm) more fault displacement necessary to initiate load transfer to the north pipe end than the south.

This additional 1.2 in. (30.5 mm) of fault displacement corresponds to an additional 0.77 in. (19.6 mm) axial test basin movement to begin load transfer to the north end. After the north end loads begin to increase, the loads at the south and north ends are in excellent agreement.

Figure 3.9 shows the average end loads vs. fault displacement. Again, neither the south nor north ends show loads until substantial movement has taken place. At an average fault displacement of 37.7 in. (958 mm) and average load of 1.2 kips (5.3 kN) there is a sharp increase in the rate at which the end loads are increasing. This "displacement transition point" corresponds to an axial basin displacement of 24.4 in. (620 mm). As discussed in Section 3.8, this transition point represents 24.4 in. (620 mm) of axial pipeline extension, which is close to the sum of the 4.5 in. (114 mm) pullout settings for the six joints.

The outside diameter of the pipe was OD = 6.65 in. (169 mm) and the average measured wall thickness was t_W = 0.34 in. (8.64 mm). This gives a pipe wall cross-sectional area of A = 6.74 in.^{2} (4348 mm^2). The average Young's modulus of the ductile iron was E = 24700 ksi (170 GPa), based on ductile iron tensile coupon tests performed at Cornell University and provided by Kubota. Using the average crown and invert strains at the gage stations and multiplying the strain times AE gives the force, F, in the pipe. The distribution of axial force along the pipe, calculated as $F = \varepsilon AE$, is shown in Figure 3.10.

Figure 3.10 shows that the axial forces in the pipe near the load cell locations are consistent with forces measured by the load cells. Both figures show that the load along the pipeline went up as the fault displacement increased. The load increased rapidly from 30 in. (762 mm) to 39 in. (991 mm) of fault displacement. All six joints attained spigot projection contact with the locking ring at 38 in. (965 mm) of fault displacement. The highest axial force was detected at the fault location, and the loads were lower at locations further away from the fault. The axial strain gages at the fault did not function properly after 30 in. (762 mm) of fault displacement.

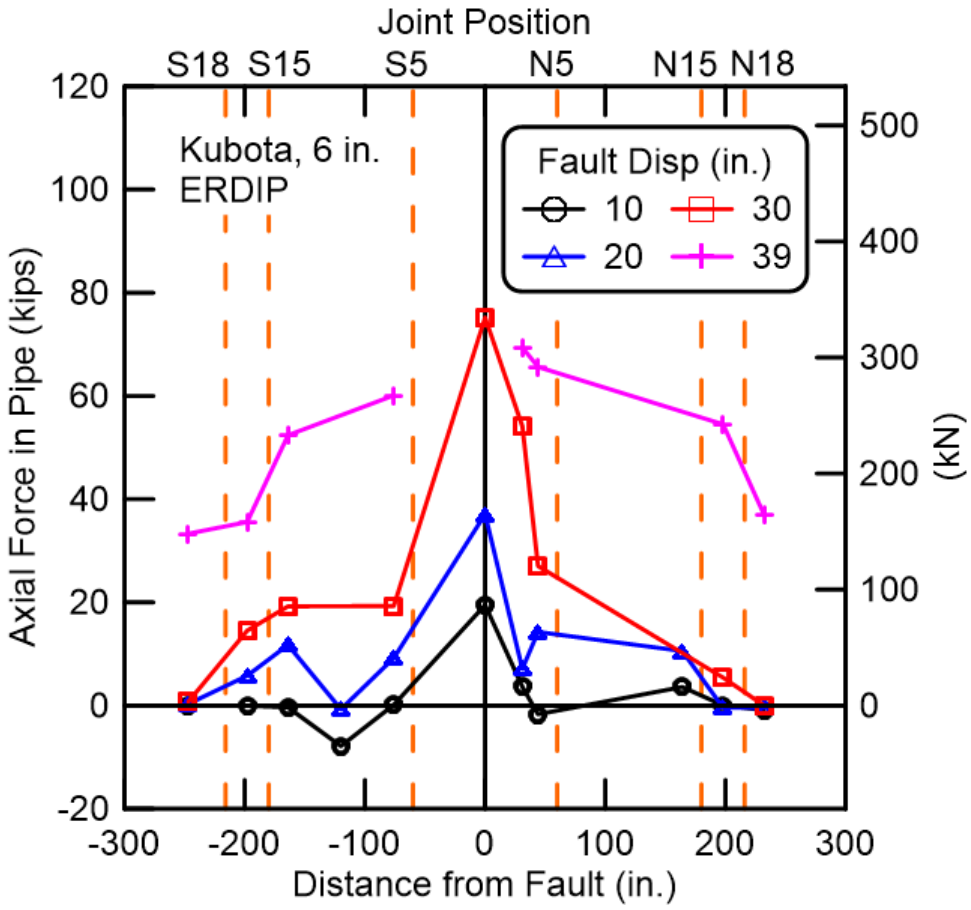

Figure 3.10. Axial Force in Pipe vs. Distance from Fault

3.8 Joint Movements and Rotations

The joint movements at the crown and east and west springlines of the S18, S15, S5, N5, N15 and N18 joints are shown in Figures 3.11 to 3.16, respectively, and the collective average movements of all joints are presented in Figure 3.17. Joint rotations are provided in Figure 3.18. The joint pullout movements and rotations were measured by the instrumentation described in Section 3.3 and shown in Table 3.2. In aggregate the measurements confirm that the pipeline was able to accommodate successfully fault rupture through axial displacements and rotations at all six joints. Moreover, the measurements provide a comprehensive and detailed understanding of how the movement was accommodated at each joint, the sequence of movements, and combined axial pullout and rotation at each joint.

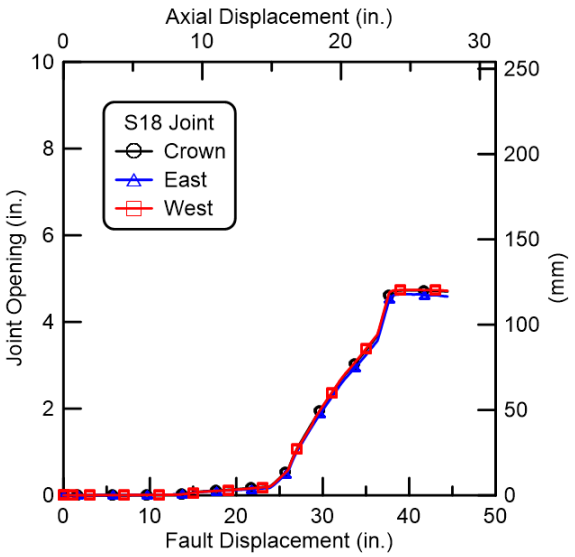

Figure 3.11. Displacements of S18 Joint

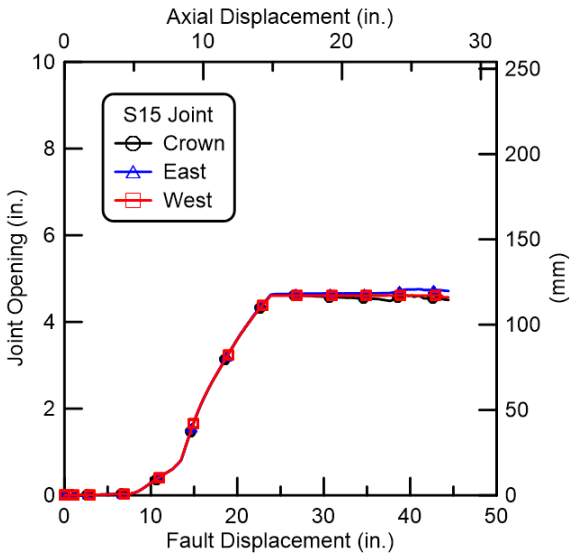

Figure 3.12. Displacements of S15 Joint

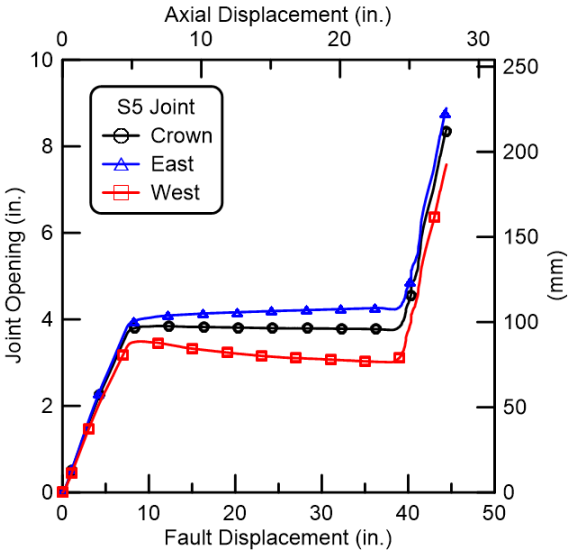

Figure 3.13. Displacements of S5 Joint

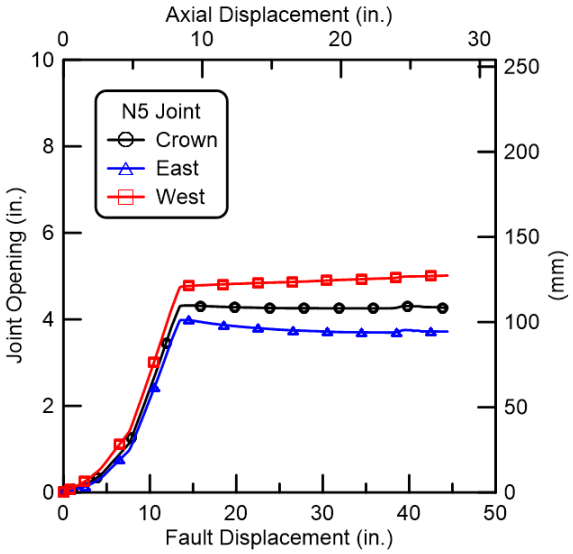

Figure 3.14. Displacements of N5 Joint

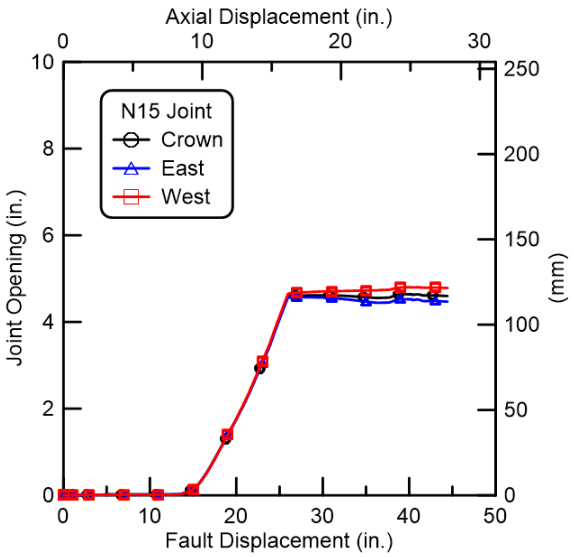

Figure 3.15. Displacements of N15 Joint

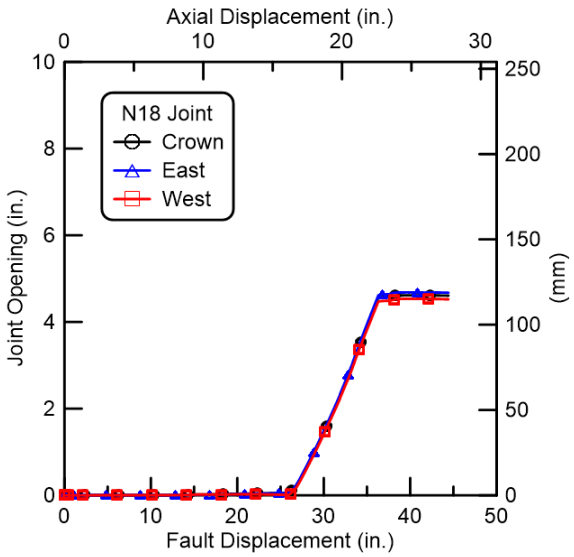

Figure 3.16. Displacements of N18 Joint

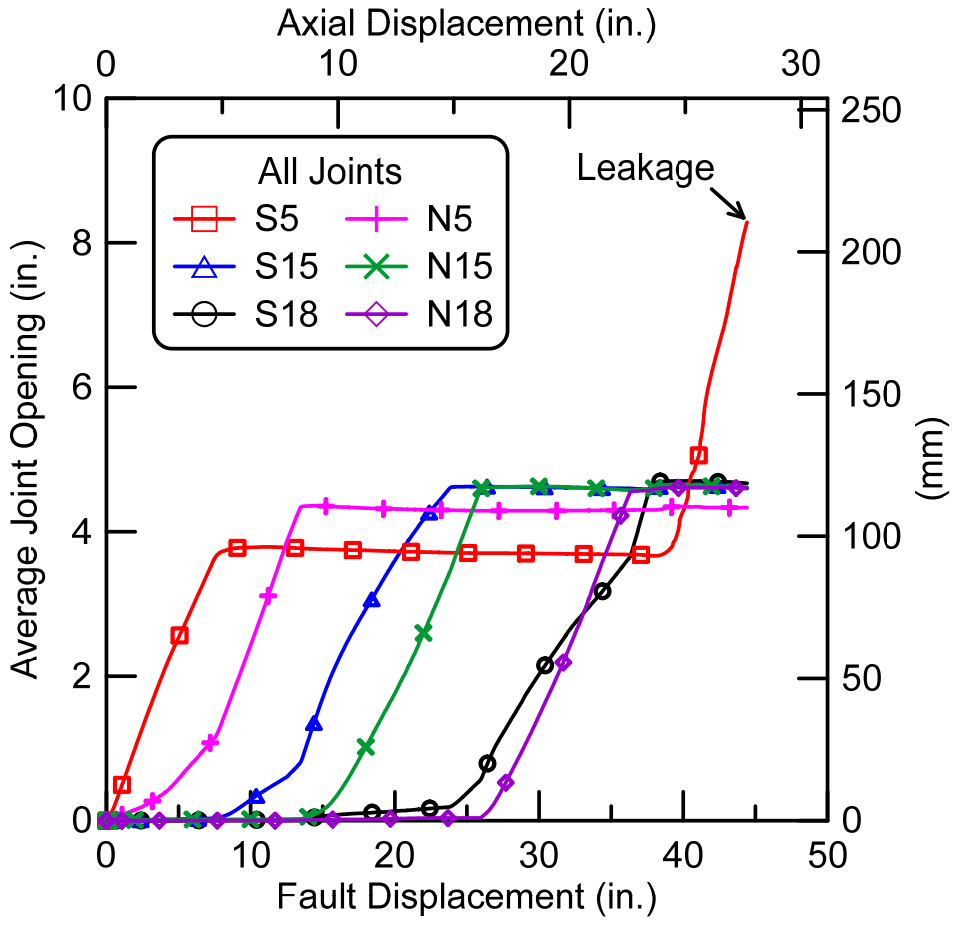

Figure 3.17. Average Joint Openings for All Joints vs. Fault Displacement

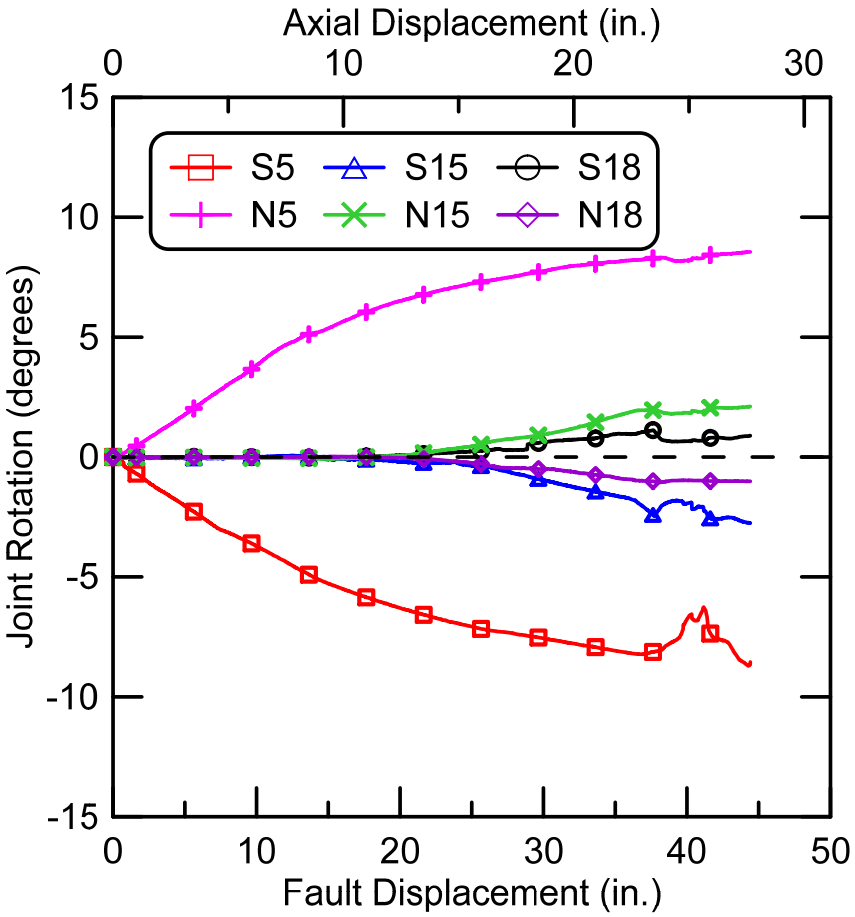

Figure 3.18. Joint Rotations vs. Fault Displacement

During the beginning part of the test, the N5 and S5 joints accommodated most of the test basin movement. The S5 joint, however, displaced faster such that the spigot projection was in contact with the locking ring at 8.0 in. (203 mm) of fault displacement. The S15 joint then began to open. At 13.4 in. (340 mm) of fault movement, the N5 joint spigot projection was engaged to its locking ring, allowing the displacement of the N15 joint. After S15 and N15 jointed were fully extended at 25.0 in. (635 mm) of fault movement, the S18 and N18 joints started opening. All six joints were extended when the fault displacement reached the 38.0 in. (965 mm) transition point (see Section 3.7), after which additional movements were measured with the largest opening at the S5 joint.

Figure 3.17 shows the average joint opening of all six joints vs. fault displacement. The S5 joint began to open first, followed by the N5, S15, N15, N18, and S18 joints, respectively. At a fault

displacement of approximately 44.4 in. (1128 mm), the S5 joint leaked, corresponding to an additional 4 in. (102 mm) of axial displacement beyond the transition point when all joints were extended to a condition of spigot projection/locking ring contact. No leakage was observed until the fault displacement reached 44.4 in. (1130 mm).

The rotations of the four joints are shown in Figure 3.18. Joint rotation is calculated from the string pot measurements at each joint as:

$$\text{Rotation}\ (\text{deg}) = \tan^{-1}\left(\frac{180}{\pi}\frac{\text{East String Pot Displacement- West String Pot Displacement}}{\text{Separation Distance between the String Pots}}\right) \quad (3.1)$$

The N5 and S5 joints, closest to the fault, had opposite joint rotations and accommodated most of the fault offset with maximum rotations of nearly 8.5 degrees. The other joint rotations were relatively small. The S15 and N15 joint rotations were approximately 2.5 degrees while the rotations at the S18 and N18 joints were about 1 degree. Figure 3.18 shows that the N and S joints beyond 5 ft did not to start to show substantial rotations until the joints were extended to full or close to full engagement.

3.9 Bending Strains

Figure 3.19 presents the measured bending strains in the pipeline, corresponding to fault displacements of 10 in. (254 mm), 20 in. (508 mm), 30 in. (762 mm), 35 in. (889 mm), and 39 in. (991 mm), respectively. The bending strains were calculated at each strain gage station as one half the difference between the springline strains. The plan view of the pipeline is similar to that in Figure 3.1, and the locations of the joints are indicated by the dashed lines.

The bending strains increase as the fault displacement becomes successively larger. In all cases, the strains are relatively low compared to the yield strain of the ductile iron pipe. The maximum measured bending strain is about 1000 με at 39 in. (991 mm) of fault displacement. When added to axial tensile strain at the location of maximum bending strain, the total maximum tensile strain is approximately 1500 με. Based on tensile coupon tests performed at Cornell University, the yield and proportional limit strains of ductile iron are 3500 με and 1200 με, respectively. Therefore, the total maximum tensile strain in the pipe during the split-basin test is less than half the yield strain, but higher than the proportional limit strain by about 25%.

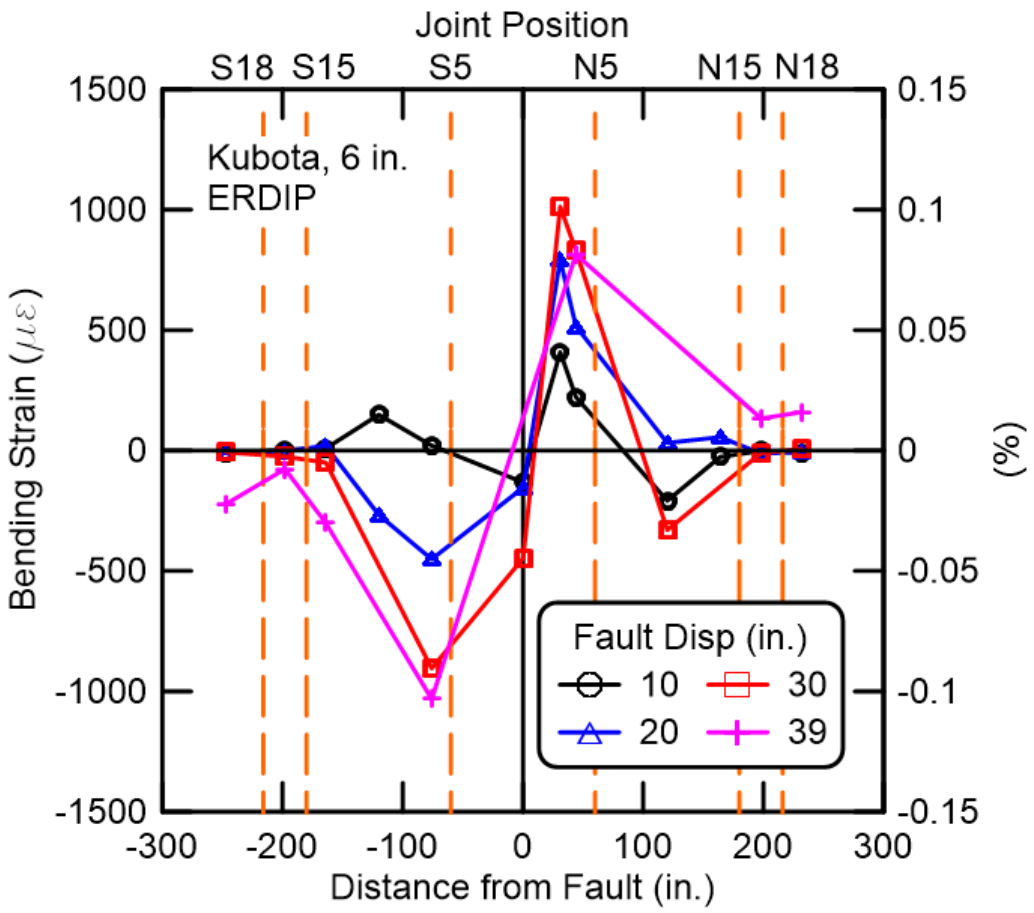

Figure 3.19. Bending Strains vs. Distance from Fault

Because bending strains and joint rotations were measured during the test, it is possible to plot the moment vs. rotation response of the south and north joints closest to the fault and compare the data with the moment vs. rotation relationship provided by Kubota during a three point bending test. Figure 3.20 presents the moment vs. rotation data for the south and north joints closest to the fault. Only moments at the bells were used because the spigot moments were affected by spigot ovaling and local irrecoverable deformations. The three point bending test was in pure bending while the moments from the split basin test were developed during simultaneous bending and tension, causing differences in the way moments and rotations were mobilized. The joints subjected to fault movement generated higher moments at lower rotations than the three point bending test joint.

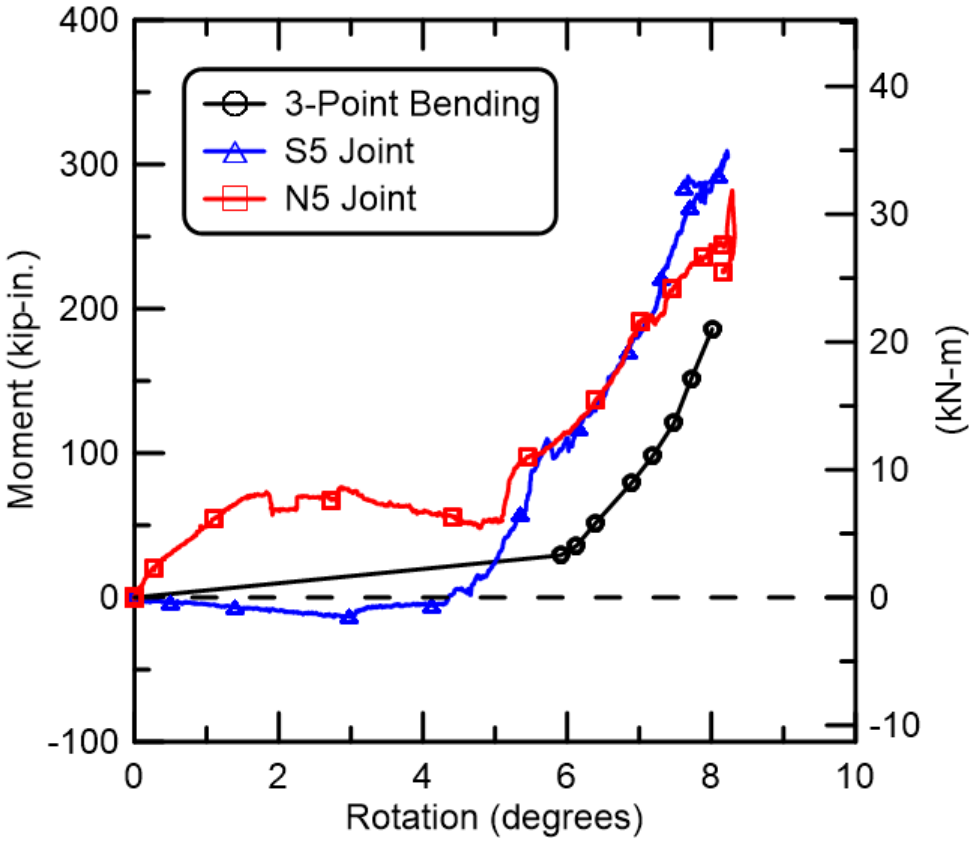

Figure 3.20. Comparison of Moment vs. Rotation Measurements during Split Basin Test with Provided Relationships during Bending Test by Kubota

3.10 Summary of Large-Scale Testing

A 40-ft (11.9-m)-long, seven-piece section of a ductile pipeline was tested at the Cornell Large-Scale Lifelines Facility. The pipe had a total of six joints. Three joints were located 5, 15, and 18 ft (1.5, 4.6, and 5.5 m) north of the fault and three joints at the same distances south of the fault. The fault angle was 50º. The pipe was instrumented with sixty-four strain gages installed at fourteen locations along the pipeline to measure strains and to evaluate axial forces and bending moments. Strain gages were positioned at the crown (C), invert (I) east (E) springline, and west (W) springline of the pipe. There were three string pots at each joint to measure joint movements and to evaluate joint rotation. Four load cells were placed outside the test basin at each end, reacting between the test basin structural frame and pipe end restraint to measure axial force. The pipe was pressurized to approximately 80 psi (552 kPa).

The pipe was placed on a bed of compacted sand, aligned, instruments checked, and then backfilled with compacted sand to a depth of cover of 30 in. (762 mm) above the pipe crown. The test basin's north section was displaced along a 50º fault at a rate of 4.8 in. (122 mm) per minute. The basin was displaced roughly 1 in. (25.4 mm), paused, and then put in motion again. At a fault displacement of 44.4 in. (1130 mm), the pipe lost pressure, and the test was stopped. No leakage was observed until the fault displacement reached 44.4 in. (1130 mm), which corresponds to 28.5 in. (725 mm) of axial extension of the test basin and pipe. Following excavation, a fracture was observed at the west springline of the spigot projection of the S5 joint.

The end forces at the south and north end of the test basin were about 30 kips (133 kN). The axial force in the pipe, as determined from the strain gage readings, was largest at 31 in. (790 mm) north of the fault at 80 kips (356 kN). It is assumed that the axial force in the pipe was at least 80 kips (356 kN).

The test measurements confirm that the pipeline was able to accommodate fault rupture through axial displacements and rotations at all six joints. Moreover, the measurements provide a comprehensive and detailed understanding of how the movement was accommodated at each joint, the sequence of movements, and combined axial pullout and rotation at each joint. The combined joint pullout displacements are 28.5 in. (725 mm), which exceeds the sum of the 4.5 in. (114 mm) spigot insertion length for all six joints. On average, the spigot at each joint pulled from the bell on the order of 4.75 in. (121 mm), thus confirming that significant additional pullout occurs beyond the slip required for the spigot projection to make contact with the locking ring. The maximum rotation measured at the joints closest to the fault was about 8.6 degrees, thus demonstrating the ability of the joints to sustain significant levels of combined axial pullout and rotation.

The Kubota earthquake resistant ductile iron pipeline was able to accommodate significant fault movement through axial pullout and rotation of the joints. Fault rupture simulated in the large-scale test is also representative of the most severe ground deformation that occurs along the margins of liquefaction-induced lateral spreads and landslides.

The amount of tensile strain that can be accommodated with the Kubota earthquake resistant ductile iron pipelines will depend on the spacing of the pipeline joints. The pipeline used in the large-scale split-basin test was able to accommodate 28.5 in. (725 mm) of axial extension, corresponding to an average tensile strain of 5.9% along the pipeline. Such extension is large

enough to accommodate the great majority of liquefaction-induced lateral ground strains measured by high resolution LiDAR after each of four major earthquakes during the recent Canterbury Earthquake Sequence in Christchurch, NZ (O'Rourke, et al., 2014). The test confirms that the Kubota ERDIPs are able to sustain without leakage large levels of ground deformation through axial displacement and rotation of its joints under full-scale conditions of abrupt ground rupture.

Section 4
Summary

Kubota has developed an earthquake-resistant ductile iron pipe (ERDIP), referred to as GENEX in Japan. Tests of 6-in. (150-mm)-diameter ERDIP pipe and pipeline section were performed at Cornell University to determine the capacity of the joint in direct tension and evaluate the ability of the jointed ductile iron pipeline to accommodate fault rupture. Test results are summarized for direct joint tension, pipeline response to fault rupture, and significance of test results under the headings that follow.

Direct Joint Tension

A tension test was performed on the 6-in. (150-mm)-diameter Kubota ERDIP joint at a maximum internal pressure of 84 psi (579 kPa). The test began with the spigot fully inserted in the bell. As the pipe was pressurized, the spigot was displaced from the bell seat at approximately 9 psi (62 kPa) internal pressure. The joint opened 4.53 in. (115 mm) before the spigot projection became engaged with the locking ring. The pipe reached a maximum axial force of 115 kips (516 kN) at an additional 0.03 in (1 mm) of displacement after ring engagement, for a total joint opening of 4.58 in. (116 mm). Forces generated between the spigot projection and locking ring sheared the spigot projection off, allowing the spigot to slip out of the bell immediately after the peak load was reached, resulting in pipe leakage.

Pipeline Response to Fault Rupture

A 40-ft (11.9-m)-long, seven-piece section of a ductile pipeline was tested at the Cornell Large-Scale Lifelines Facility. The pipe had a total of six joints. Three joints were located 5, 15, and 18 ft (1.5, 4.6, and 5.5 m) north of the fault, and three joints were located at the same distances south of the fault. The fault angle was 50º. The pipe was pressurized to approximately 80 psi (552 kPa). The pipe was placed on a bed of compacted partially saturated sand, aligned, instruments checked, and then backfilled with compacted sand to a depth of cover of 30 in. (0.76 m) above the pipe crown. The test basin's north section was displaced along a 50º fault at a rate of 4.8 in. (122 mm) per minute. At a fault displacement of 44.4 in. (1130 mm), the pipe lost pressure, and the test was stopped. The 44.4 in. (1130 mm) fault displacement corresponds to 28.5 in. (725 mm) of axial extension of the test basin and pipe. Following excavation, a fracture was observed at the west

springline of the spigot projection of the S5 joint.

The test measurements confirm that the pipeline was able to accommodate successfully fault rupture through axial displacements and rotations at all six joints. Moreover, the measurements provide a comprehensive and detailed understanding of how the movement was accommodated at each joint, the sequence of movements, and combined axial pullout and rotation at each joint. The combined joint pullout displacements are 28.5 in. (725 mm), which exceeds the sum of the 4.5 in. (114 mm) spigot insertion length for all six joints. On average, the spigot at each joint pulled from the bell on the order of 4.75 in. (121 mm), thus confirming that significant additional pullout occurs beyond the slip required for the spigot projection to make contact with the locking ring. The maximum rotation measured at the joints closest to the fault was about 8.5 degrees.

Significance of Test Results

Large-scale fault rupture tests at Cornell demonstrate the ability of the Kubota ERDIP joints to accommodate significant fault movement through axial pullout and rotation of the joints. Fault rupture simulated in the large-scale test is also representative of the most severe ground deformation that occurs along the margins of liquefaction-induced lateral spreads and landslides.

The amount of tensile strain that can be accommodated with the Kubota earthquake resistant ductile iron pipelines will depend on the spacing of the pipeline joints. The pipeline used in the large-scale split-basin test was able to accommodate 28.5 in. (725 mm) of axial extension, corresponding to an average tensile strain of 5.9% along the pipeline. Such extension is large enough to accommodate the great majority (over 99%) of liquefaction-induced lateral ground strains measured by high resolution LiDAR after each of four major earthquakes during the recent Canterbury Earthquake Sequence (CES) in Christchurch, NZ (O'Rourke, et al., 2014).. These high resolution LiDAR measurements for the first time provide a comprehensive basis for quantifying the ground strains caused by liquefaction on a regional basis. To put the CES ground strains in perspective, the levels of liquefaction-induced ground deformation measured in Christchurch exceed those documented in San Francisco during the 1989 Loma Prieta earthquake and in the San Fernando Valley during the 1994 Northridge earthquake. They are comparable to the levels of most severe liquefaction-induced ground deformation documented for the 1906 San Francisco earthquake, which caused extensive damage to the San Francisco water distribution system. The tests confirm that the Kubota ERDIP joints are able to sustain without leakage large levels of

ground deformation, the magnitude of which will vary depending on the ground deformation patterns and spacing of the joints.

References

ASTM International (2013). "Standard Test Methods for Tension Testing of Metallic Materials", *ASTM Standards*. E8/E8M - 13a, 1 – 28.

AWWA (2009). "Ductile Iron Pipe, Centrifugally Cast for Water", *AWWA Standard*. ANSI/AWWA C151/A21.51-09.

O'Rourke, T.D. (1998). "An Overview of Geotechnical and Lifeline Earthquake Engineering", Geotechnical Special Publication No. 75, ASCE, Reston, VA, Proceedings of Geotechnical Earthquake Engineering and Soil Dynamics Conference, Seattle, WA, Aug. 1998, Vol. 2, pp.1392-1426.

O'Rourke, T.D. and J.W. Pease (1997). "Mapping Liquefiable Layer Thickness for Seismic Hazard Assessment", Journal of Geotechnical Engineering, ASCE, New York, NY, Vol. 123, No.1, January, pp. 46-56.

O'Rourke, T.D., A. Bonneau, J. Pease, P. Shi, and Y. Wang (2006). "Liquefaction Ground Failures in San Francisco" Earthquake Spectra, EERI, Oakland, CA, Special 1906 San Francisco Earthquake Vol. 22, No. 52, Apr., pp. 691-6112.

O'Rourke, T.D., Jeon, S-S., Toprak, S., Cubrinovski, M., Hughes, M., van Ballegooy, S., and Bouziou, D. (2014) "Earthquake Response of Underground Pipeline Networks in Christchurch, NZ", Earthquake Spectra, EERI, Vol. 30, No.1, pp. 183-204**.**

Pease, J.W. and T.D. O'Rourke (1997), "Seismic Response of Liquefaction Sites", Journal of Geotechnical Engineering, ASCE, New York, NY, Vol. 123, No. 1, January, pp. 37-45.